Japanese Journal of Applied Physics
Vol. 45, No. 9, 2006, pp. L265–L267

Magnetic Structure of Y-shaped Permalloy Arrays Fabricated Using Damascene Technique

Kenji MACHIDA[1,2], Takahiro YAMAMOTO[2], Takehiro YAMAOKA[3], Takayuki ISHIBASHI[2] and Katsuaki SATO[2]

[1]*Materials Science, Science & Technical Research Laboratories, NHK, 1-10-11 Kinuta, Setagaya-ku, Tokyo 157-8510, Japan*
[2]*Faculty of Technology, Tokyo University of Agriculture and Technology, 2-24-16 Nakacho, Koganei, Tokyo 184-8588, Japan*
[3]*Application Engineering, SII NanoTechnology, Inc., 2-15-5 Shintomi, Chuo-ku, Tokyo 104-0041, Japan*

(Received November 8, 2005; accepted January 12, 2006; published online February 24, 2006)

In this paper, we report on the observed magnetic spin structure and the micromagnetic simulation of Y-shaped permalloy ($Ni_{80}Fe_{20}$) arrays. The arrays were fabricated using the damascene technique, with electron-beam lithography. For a widely separated linear arrangement, magnetic poles are observed on the ends of two of three arms of the Y-shaped array and multidomains on the remaining arm. For a closely separated honeycomb arrangement and a pair of antisymmetrical dots (termed mirror dots), regularly aligned magnetic poles are observed. It is suggested that the honeycomb array or mirror dots have a strong magnetostatic interaction. The calculated spin distributions approximately correspond to the magnetic force microscopy (MFM) images, in good agreement with the experimental results. [DOI: 10.1143/JJAP.45.L265]

KEYWORDS: damascene technique, electron-beam lithography, magnetic structure, micromagnetic simulation, magnetic force microscopy

It is critical to understand the magnetic spin structures and magnetic switching behaviors of nanoscale patterned magnetic elements for their application in high-density data storage devices, nonvolatile magnetic memories, and magnetic logic gates. The spin structures of magnetic dots have been extensively studied.[1)] We have investigated regularly aligned magnetic arrays of square, rectangular, circular, and cross-shaped permalloy ($Ni_{80}Fe_{20}$) dots embedded in silicon wafers.[2–4)] These patterns were successfully fabricated using the damascene technique, with electron-beam (EB) lithography. In this paper, we focused on a regularly aligned array of Y-shaped permalloy dots with three arms of 300 nm or 200 nm in width and investigated their spin structures using magnetic force microscopy (MFM) and micromagnetic simulation.

Figure 1(a) shows a scanning electron microscopy (SEM) micrograph of a regularly aligned Y-shaped permalloy array with a linear arrangement (widely separated) and Fig. 1(b) shows a honeycomb arrangement (closely separated). One of the arms in the Y-shaped dot is 1.4 μm in length and 300 nm in width. The relative distance among adjacent dots is as long as 6 μm for the widely separated arrangement. The separation of the dots is 400 nm for the closely separated arrangement. The arrays were fabricated on a Si(100) wafer using EB lithography. EB resist films (ZEP520A-7 supplied by Nippon Zeon Co., Ltd.) were spin-coated on the wafer at a constant speed of 5000 rpm for 60 s, followed by baking at 180 °C for 2 min. The resist films were exposed using an EB lithography system (Elionix type ELS-7300ULH). The electron accelerating voltage was 30 kV, and the exposure radiation dose was 216 μC/cm^2. The exposed resist films were developed using a ZED-N50 (n-Amyl acetate) developer for 30 s at 24 °C.

The wafer coated with the patterned resist films was dry-etched using CF_4 gas with RF power of 400 W for 90 s, and pit arrays of approximately 130 nm in depth were formed on the wafer. The remanent resist was removed by acetone, and permalloy films were deposited using an EB evaporator so as to fill the pit arrays. The deposition rate was approximately 0.5 Å/s. The films outside the pit were subjected to a chemical mechanical polishing (CMP) with slurry (GLANZOX SP-15 supplied by Fujimi Corp.) to obtain a flat surface. The surface roughness after CMP was 0.9 nm (rms).

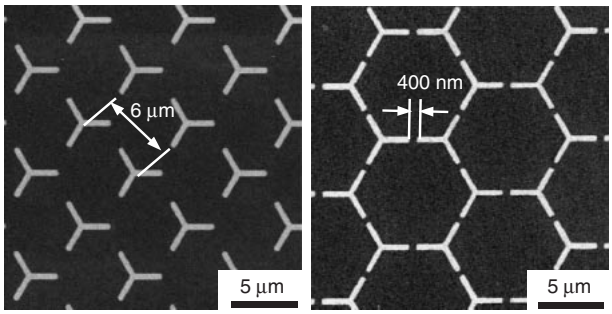

Fig. 1. SEM images for regularly aligned arrays of Y-shaped permalloy dots with (a) linear arrangement and (b) honeycomb arrangement.

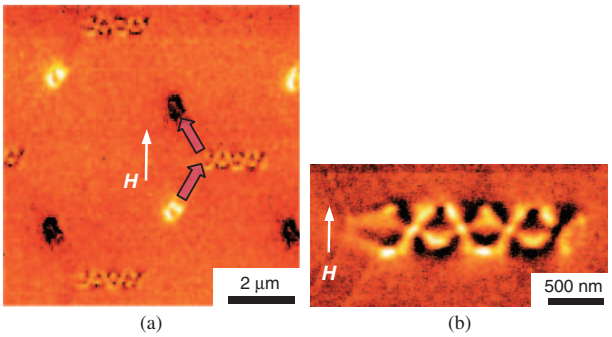

Fig. 2. (a) MFM image for widely separated linear array of Y-shaped dots and (b) magnified image in arm with multidomain structure, after applying H of 80 Oe.

The remanent state was observed using an SII Nanotechnology model SPI4000 Nano-Navi/E-sweep MFM system with a low-moment probe (having a 24-nm-thick Co–Cr–Pt-coated tip). The system has a quality factor (Q) control which is specially designed for highly sensitive detection in high vacuum.[5)]

Figure 2(a) shows an MFM image of the widely separated array of the Y-shaped dots, after applying a magnetic field (H) of 80 Oe. Magnetic poles are observed at the ends of two of the three arms. The observed magnetic pole represents a single-domain structure in the arm. On the contrary, a

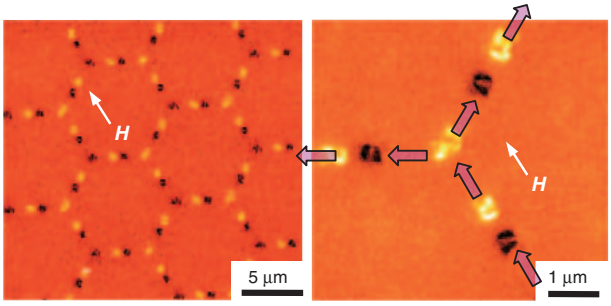

Fig. 3. (a) MFM image of closely separated honeycomb array of Y-shaped dots and (b) magnified image of specific dot with arrows showing spin flows in each arm, after applying H of 80 Oe.

multidomain structure appears on the remaining arm, for which the magnified MFM image is given in Fig. 2(b). The alignment rule of a couple of single domains and the other multidomain is found to be just the same in all dots, as shown in Fig. 2(a). However, the directions of magnetizations (spin flows) in the single domains are reversed by an applied H as small as 80 Oe. After demagnetization, the positions of the single-domain arms and the multidomain arm in each Y-shaped dot are not necessarily aligned in order; a completely random arrangement is observed.

Figure 3(a) shows an MFM image of the closely separated array and Fig. 3(b) shows a magnified image of a specific dot, after applying an H of 80 Oe. Regularly aligned black and white spots are observed at the end of each arm. The spin flow is found to satisfy the "two in, one out" or the "one in, two out" rule around the vertex, similar to the case described in ref. 6. In the closely separated array, the spin flows in the arms are not reversed by an applied H of 80 Oe, unlike in the case of the widely separated array. The difference in spin structures between the widely and closely separated arrangements is assumed to be due to a strong magnetostatic interaction.

The micromagnetic simulator[7] based on the Landau–Lifshitz–Gilbert equation was modified to correspond to a three-dimensional pattern. The equation was numerically solved using the fourth-order Runge–Kutta method for high accuracy. The MFM output signals are proportional to the force gradient between the tip and the sample. The force gradient is given by[8]

$$\frac{\delta F_z}{\delta z_{\mathrm{tip}}} = \int_{\mathrm{sample}} \frac{\partial^2 \boldsymbol{H}_{\mathrm{tip}}}{\partial z^2} \boldsymbol{M}_{\mathrm{sample}} d^3 r + \int_{\mathrm{sample}} \frac{\partial \boldsymbol{H}_{\mathrm{tip}}}{\partial z} \cdot \frac{\delta \boldsymbol{M}_{\mathrm{sample}}}{\delta z_{\mathrm{tip}}} d^3 r, \quad (1)$$

where $\boldsymbol{H}_{\mathrm{tip}}$ is the stray field from the tip at a sample volume element, $\boldsymbol{M}_{\mathrm{sample}}$ is the magnetization of the element at equilibrium, and z_{tip} is the tip-sample distance. The distributions of $\boldsymbol{H}_{\mathrm{tip}}$ were calculated by an integral equation method. $\delta \boldsymbol{M}_{\mathrm{sample}}/\delta z_{\mathrm{tip}}$ in the second term is considerable. However, in this work, this term was excluded to save calculation time.

Figure 4(a) shows the magnetization configuration of an isolated Y-shaped dot (300 nm in width, 1.4 μm in arm length, and 100 nm in depth); the dot has approximately the same size as that shown in Fig. 1, which was calculated without considering magnetostatic interactions among adjacent dots. The elementary volume is $25 \times 25 \times 25\,\mathrm{nm}^3$. The saturation magnetization is $800\,\mathrm{emu/cm}^3$. The exchange stiffness constant, gyromagnetic constant, and damping constant are $1.3 \times 10^{-6}\,\mathrm{erg/cm}$, $-1.76 \times 10^7\,\mathrm{rad/(s \cdot Oe)}$, and 0.1, respectively. According to in-plane magnetization curves, the evaporated permalloy films are isotropic. Consequently, the uniaxial anisotropic constant was set to $10\,\mathrm{erg/cm}^3$ with the easy axis in the x-direction. Single domains appeared in the two arms and a multidomain structure composed of four chained closer domains on the remaining arm, respectively. The spin flow at the crossing region formed by the intersection of three arms turns left in two steps. Figure 4(b) shows the calculated z-component force gradient distribution, which is in good agreement with the MFM image shown in Fig. 2(b).

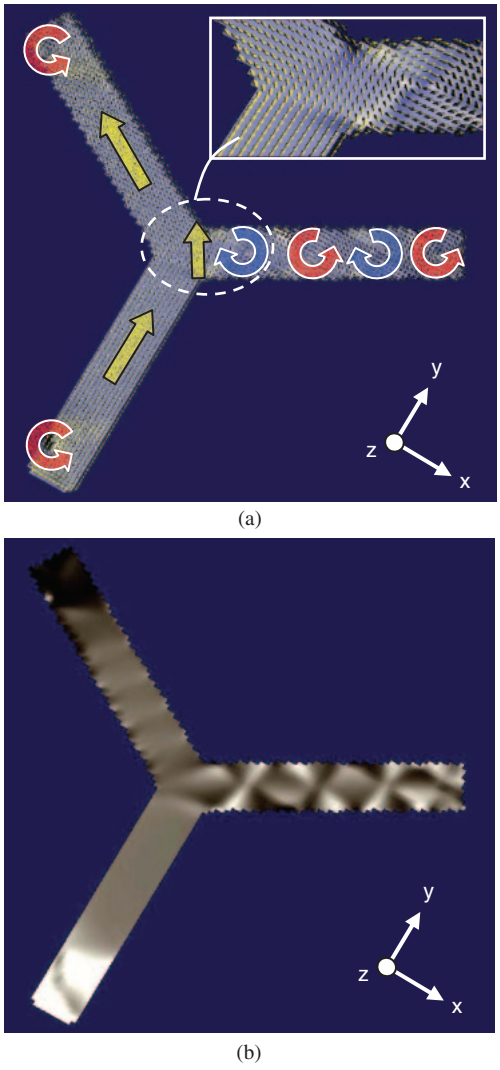

Fig. 4. (a) Calculated magnetization configuration of isolated Y-shaped permalloy dot, and (b) z-component force gradient distribution.

As shown in Fig. 5(a), the regularly aligned array for another pattern of Y-shaped permalloy dots (termed mirror dots) was fabricated; the unit structure of the array is composed of a pair of antisymmetrical dots (200 nm in width, 1.4 μm in arm length, and 50 nm in depth) separated by 400 nm as shown in Fig. 5(b). The array was formed

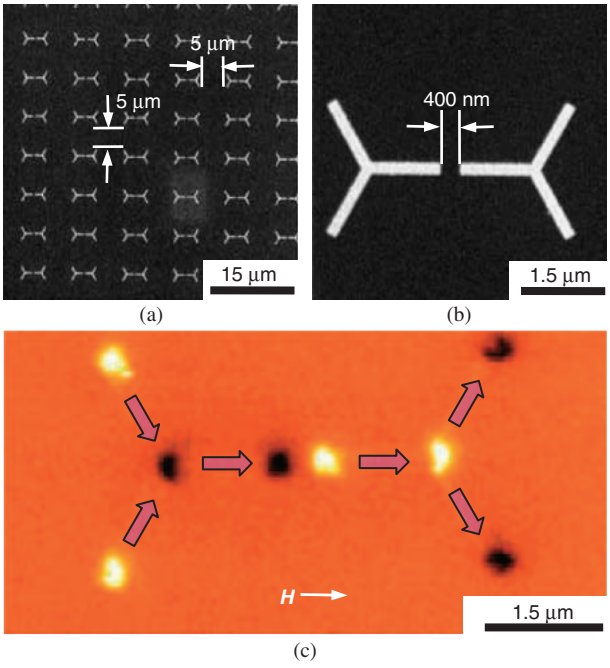

Fig. 5. (a) SEM micrograph for regularly aliened array of Y-shaped permalloy mirror dots and (b) magnified image. (c) MFM image of mirror dots with arrows showing spin flows in each arm, after applying H of 100 Oe during deposition of permalloy.

using an ultrahigh-precision EB lithography system (Elionix type ELS-7000). An MFM image taken after applying an H of 100 Oe during a deposition of permalloy is shown in Fig. 5(c). The same number of black and white spots appeared in each dot, of which the positions were aligned antisymmetrically. Estimated spin flows are shown by arrows in Fig. 5(c).

Subsequently, a micromagnetic simulation was carried out for the mirror dots. Figure 6(a) shows the magnetization configuration of the dots (200 nm in width, 1.4 μm in arm length, and 40 nm in depth), which have approximately the same size as those shown in Fig. 5. In this case, the elementary volume is a $20 \times 20 \times 20\,\mathrm{nm}^3$. Calculated spin flows similar to the above-mentioned experimental results are obtained. It is found that the vortices with the same direction of rotation (chirality) in each dot appear at the ends of all arms. The chirality of the adjacent dot shows a mirror reflection, suggesting the existence of a significant magnetostatic interaction in the mirror dots. Figure 6(b) shows the calculated z-component force gradient distribution. The same number of black and white spots appeared in each dot, with complete correspondence to the experimental MFM image shown in Fig. 5(c).

In conclusion, regularly aligned arrays of Y-shaped permalloy dots were fabricated using the damascene technique and their spin structures were investigated using MFM measurements and a micromagnetic simulation. For widely separated alignment, magnetic poles are observed at the ends of two arms, and multidomains on the remaining arm. For closely separated alignment and mirror dot arrays, regularly aligned magnetic poles are observed. It is suggested that closely separated or mirror dot arrays have

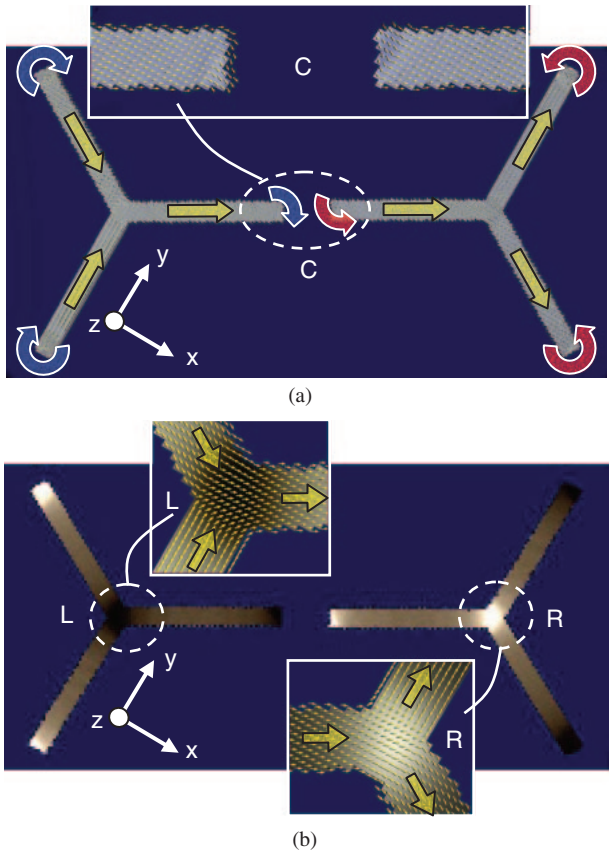

Fig. 6. (a) Calculated magnetization configurations of Y-shaped permalloy mirror dots with magnified image of arms separated by 400 nm, and (b) z-component force gradient distributions with magnified images for crossing regions formed by intersections of three arms.

a significant magnetostatic interaction. The calculated spin structures approximately correspond to the MFM images, in good agreement with the experimental results.

Acknowledgments

The authors are very grateful to Mr. Y. Taguchi and Mr. K. Terabun of Elionix Inc. for permission to use the ultrahigh-precision electron-beam lithography system, ELS-7000. This research has been conducted under the 21st century COE program of Tokyo University of Agriculture and Technology on “Future Nano Materials”.

1) A. Hubert and R. Schäefer: *Magnetic Domains—The Analysis of Magnetic Microstructures* (Springer, New York, 1998) p. 463.
2) T. Matsumoto, T. Tezuka, T. Ishibashi, Y. Morishita, A. Koukitu and K. Sato: Trans. Magn. Soc. Jpn. **3** (2003) 103.
3) T. Tezuka, T. Yamamoto, K. Machida, S. Shimizu, T. Ishibashi, Y. Morishita, A. Koukitu and K. Sato: Trans. Magn. Soc. Jpn. **4** (2004) 241.
4) K. Machida, T. Tezuka, T. Yamamoto, T. Ishibashi, Y. Morishita, A. Koukitu and K. Sato: J. Magn. Magn. Mater. **290–291** (2005) 779.
5) T. Yamaoka, K. Watanabe, Y. Shirakawabe and K. Chinone: J. Magn. Soc. Jpn. **27** (2003) 429 [in Japanese].
6) E. Saitoh, M. Tanaka and H. Miyajima: J. Appl. Phys. **93** (2003) 7444.
7) K. Machida, N. Hayashi, Y. Yoneda, J. Numazawa, M. Kohro and T. Tanabe: J. Magn. Magn. Mater. **226–230** (2001) 2054.
8) J. M. García, A. Thiaville, J. Miltat, K. J. Kirk, J. N. Chapman and F. Alouges: Appl. Phys. Lett. **79** (2001) 656.